

MAViL: Masked Audio-Video Learners

Po-Yao Huang Vasu Sharma Hu Xu Chaitanya Ryali Haoqi Fan Yanghao Li Shang-Wen Li Gargi Ghosh
Jitendra Malik Christoph Feichtenhofer
Meta AI, FAIR

Abstract

We present Masked Audio-Video Learners (MAViL) to train audio-visual representations. Our approach learns with three complementary forms of self-supervision: (1) reconstruction of masked audio and video input data, (2) intra- and inter-modal contrastive learning with masking, and (3) self-training by reconstructing joint audio-video contextualized features learned from the first two objectives. Pre-training with MAViL not only enables the model to perform well in audio-visual classification and retrieval tasks but also improves representations of each modality in isolation, without using information from the other modality for fine-tuning or inference. Empirically, MAViL sets a new state-of-the-art on AudioSet (53.1 mAP) and VGGSound (67.1% accuracy). For the first time, a self-supervised audio-visual model outperforms ones that use external supervision on these benchmarks.

1. Introduction

We study self-supervised representation learning from audio and video, two rich, heterogeneous, yet closely related modalities of human perception. Self-supervised learning (SSL) with Transformers (Vaswani et al., 2017; Paulus et al., 2017) has revolutionized many research areas. There are mainly two types self-supervision: reconstruction and contrastive learning. In natural language processing (NLP), BERT (Devlin et al., 2019) pre-training by performing masked prediction on large-scale language corpora has refreshed the leaderboards of many NLP tasks. For other modalities, masked autoencoders (MAE) have effectively learned uni-modality representations by reconstructing images (He et al., 2022), video (Feichtenhofer et al., 2022), and audio (Huang et al., 2022a). On the other hand, contrastive learning is popular to learn cross-modality alignment in language-image (Radford et al., 2021) or audio-visual (Owens & Efros, 2018) tasks.

In this work, we investigate a unifying methodology where masked autoencoding meets contrastive objectives for learn-

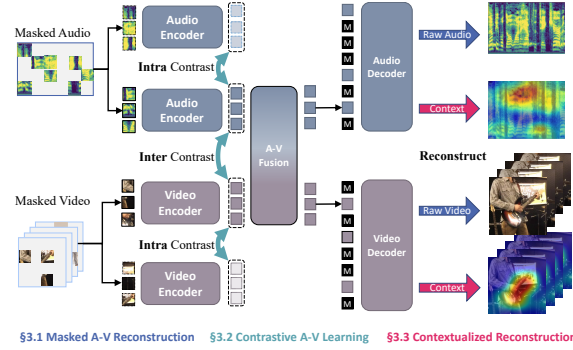


Figure 1. **Masked Audio-Video Learners (MAViL)**. We introduce three multimodal objectives for learning complementary audio-video representations: (1) Masked audio-video reconstruction; (2) Masked inter-modal and intra-modal contrastive learning; (3) Masked self-training on contextualized multimodal features. MAViL not only learns strong joint audio-video representations, but can also improve single modality encoders, *without* using the other modality during fine-tuning or inference.

ing audio-video representations. Besides targeting strong joint representations for audio-video tasks, we are also interested in uni-modal advances; *e.g.*, for audio-only tasks, we envision that an audio encoder would work better if it learns also from video over only from audio.

We present Masked Audio-Video Learners (MAViL). Our model consists of an audio-visual encoder pair, a shallow fusion-encoder layer to connect and exchange multimodal information, and separate decoders for reconstructing raw inputs and contextualized features, as illustrated in Fig. 1. We train MAViL using three objectives outlined next.

First, we reconstruct information that has been removed by applying a high masking ratio (*e.g.* 80%) to the input (He et al., 2022; Feichtenhofer et al., 2022; Huang et al., 2022a). With this, MAViL learns *complementary* audio-video representations by reconstructing a single modality, with the supplementary context from the other.

Second, to utilize natural audio-visual correspondences in videos, we employ contrastive objectives (Gutmann & Hyvärinen, 2010; van den Oord et al., 2018) to learn an *aligned* latent space where an audio and a video clip are close to each other if they are spatiotemporally/audiovisually corresponding (*e.g.*, from the same instance) and enforce dis-

tance in embeddings for non-corresponding pairs. MAViL uses two forms of contrastive alignment. (i) A cross-modal objective that pulls together video and audio from the same sample and contrasts it with other samples (*i.e.* inter-modal contrast). (ii) A within-modal objective, that generates two complementary masks per modality and then pulls together encoder embeddings from the same instance, while contrasting it with embeddings from other instances of the same modality (*i.e.* intra-modal contrast). Our experiments show that both inter- and intra-modal contrastive learning contribute to stronger representations.

Third, to learn both *complementary* and *aligned* audio-video representations, we go beyond reconstructing *heterogeneous*, uni-modal raw inputs (audio *or* video) and introduce a new pre-training objective that reconstructs *homogeneous* contextualized features in a *joint* audio-video latent space.

We are motivated by the recent successes in visual SSL that use disparate teacher models to generate contextualized features as reconstruction targets. For example, BEiT (Bao et al., 2021) uses features by DALL-E (Ramesh et al., 2021) as its target. MaskFeat (Wei et al., 2022a) predicts masked target features such as HOG (Dalal & Triggs, 2005) or DINO (Caron et al., 2021). Inspired by these uni-modal teachers, we take a step further to propose a new masked *multimodal contextualized reconstruction* pretext task. Our core idea is: instead of predicting raw inputs in heterogeneous modalities, the model with masked-view inputs jointly predicts contextualized representations in the homogeneous *audio-video latent space* generated by a teacher (*i.e.* an identical model pre-trained with the masked reconstruction and contrastive objectives above) with complete-view inputs in all modalities. This approach ensures the students learn well-aligned and contextualized audio-video representations and thus improves its performance on downstream tasks. To achieve this without relying on external teacher models, we use a simple two-stage self-training framework (illustrated in Fig. 2). In the 1st stage, we train the teacher MAViL and use raw inputs as its reconstruction targets. In the 2nd stage, the student MAViL (the final model for later fine-tuning) learns to reconstruct the contextualized features output by the fusion encoder of the teacher.

Experiments on audio-video classification and retrieval tasks validate the effectiveness of our methods. We show that audio-video pre-training significantly outperforms audio-only pre-training. MAViL surpasses self-supervised benchmarks and is on par with the best supervised pre-trained model. Specifically, MAViL achieves a new state-of-the-art (audio-only and audio-video) for classification on AudioSet (48.4 and 53.1 mAP) and VGGSound (60.8 and 67.1 Acc), as well as on audio-to-video retrieval in VTT (23.5 R@1) and YouCook (33.0 R@1).

In summary, this paper presents MAViL to learn a joint audio-visual representation by reconstructing masked audio and video inputs, contrasting inter-modal and intra-modal embeddings, as well contextualized self-training on joint audio-video latents from a previously learned model. MAViL outperforms the prior state-of-the-art on AudioSet and VGGSound classification as well as audio-to-video retrieval on VTT and YouCook.

2. Related Work

Supervised Audio-Video Models. Inspired by the fact that infants pick up a language and learn their understanding about the world by relying on visual signals and co-occurring audio events (Roy, 1999), research on audio-visual learning has a long history (Ramachandram & Taylor, 2017; Chrupala, 2022). Audio-video automatic speech recognition (ASR) (Petajan, 1984; Chen & Rao, 1998; Potamianos et al., 2003) and person identification (Aleksic & Katsaggelos, 2006) have been studied before the deep learning era. Advances in deep learning enabled progress in supervised audio and audio-video tasks (Ngiam et al., 2011; Kim et al., 2013; Ephrat et al., 2018; Kazakos et al., 2019; Xiao et al., 2020; Chen et al., 2020; Nagrani et al., 2021; Koutini et al., 2021; Chen et al., 2022). However, deep learning techniques are data and annotation hungry. Although there are efforts to collect large-scale, labeled datasets in certain audio-video tasks (Harwath et al., 2018), the dependency on heavy investment in annotation slows down the application of advancements in modeling to more tasks. In comparison, MAViL relies on no labeled data.

Self-Supervised Audio-Video Representation Learning.

To alleviate annotation effort and better exploit unlabeled audio-video content abundant on the Internet, a considerable body of researches explore self-supervised techniques for learning audio-video representations (Aytar et al., 2016; Arandjelovic & Zisserman, 2017; 2018; Korbar et al., 2018; Shi et al., 2022). Similar to the popular CLIP (Radford et al., 2021) model for image-text, inter-modal contrastive learning has been studied to associate views from paired audio-video instances as self-supervision (Ma et al., 2020; Owens & Efros, 2018; Morgado et al., 2021b; Patrick et al., 2021b). Data augmentation (Patrick et al., 2021a; Wang et al., 2021) and methods for mining harder negatives (Zeng et al., 2021; Recasens et al., 2021; Morgado et al., 2021a) have been studied to improve performance. MAViL integrates masked auto-encoding and contrastive learning. We noticed another independent and concurrent study CAV-MAE (Gong et al., 2022b) also leverages MAE (He et al., 2022) and inter-modal contrastive objective (Huang et al., 2022b). Compared to theirs, MAViL additionally facilitates intra-modal contrastive and promotes multimodal contextualized reconstruction that deliver superior performance.

Knowledge Distillation KD (Hinton et al., 2015; Tian et al., 2019; Park et al., 2019b) or student-teacher learning was initially designed for model compression (Romero et al., 2015; Mishra & Marr, 2018; Cho & Hariharan, 2019). Recently, KD is gaining attention in the context of SSL, including learning better distribution of SSL representation (Wei et al., 2022c) by distilling/reconstructing teacher’s contextualized features (Grill et al., 2020; Bao et al., 2021; Wei et al., 2022b). MoCo (He et al., 2020), DINO (Caron et al., 2021), and dBOT (Liu et al., 2022) leverage self-distillation to bootstrap targets from model snapshots in previous pre-training steps. Data2vec (Baevski et al., 2022) performs self-distillation in disparate modalities, where each one bootstraps targets separately. MaskFeat (Wei et al., 2022a) pre-trains by prediction of masked target features such as HOG (Dalal & Triggs, 2005) or DINO. In contrast, MAViL is the first work that employs multimodal self-distillation with MAE. It uniquely incorporates complete-view multimodal fusion in the teacher network while the students take masked-view inputs.

3. Masked Audio-Video Learners

We introduce Masked Audio-Video Learners (MAViL), a self-supervised audio-video representation learning framework illustrated in Fig. 1. Our framework consists of two stages: In the 1st stage, MAViL learns to reconstruct spectrogram and pixels simultaneously by exploiting complementary information from each modality (§3.1), and couples this with contrastive learning to encourage intermediate (inter-/intra-)modal alignments of semantically similar audio and video pairs (§3.2). In the 2nd stage, as illustrated in Fig. 2, we use the first-stage model trained with raw targets as the teacher. We use its contextualized features to guide the student in self-training (§3.3). In the following, we describe these three types of supervision in detail and start by discussing MAViL trained with raw inputs.

3.1. Masked Uni-Modal Reconstruction

Since perception naturally involves processing visual and acoustic information jointly, MAViL uses a fusion encoder to learn joint audio-visual latents in a multimodal Transformer and uses the complementary information from each modality to reconstruct raw audio and video simultaneously. This is different from uni-modal MAE approaches (e.g. MAE (He et al., 2022), Audio-MAE (Huang et al., 2022a), or Video-MAE (Feichtenhofer et al., 2022)).

Specifically, given an audio-video pair $(a, v) \in \mathcal{D}$, we first patchify/tokenize spectrogram and video frame pixels into audio and visual tokens with uni-modal patch-embedding layers into $\mathbf{a} = [a_1 \dots a_N]$ for spectrogram and $\mathbf{v} = [v_1 \dots v_M]$, where $a_i, v_j \in \mathbb{R}^H$ for RGB patches. This is achieved via applying (FFT/video) transform(s), 2D-

convolutional layer, and flattening. Similar to MAE (He et al., 2022), we add fixed 2-D sinusoidal positional embeddings to the embedded patches for each modality. For masked audio-video reconstruction, we randomly mask the majority (i.e. 80%) of audio and video tokens and only feed the 20% unmasked audio tokens \mathbf{a}' and video tokens \mathbf{v}' to the audio encoder $f_a(\cdot)$ and the video encoder $f_v(\cdot)$, respectively. The resulting uni-modal embedding is denoted as $\mathbf{a}_{\text{um}} = f_a(\mathbf{a}')$ and $\mathbf{v}_{\text{um}} = f_v(\mathbf{v}')$.

We follow our uni-modal encoders with a multimodal *fusion* encoder. We investigate two Transformer variants as the joint fusion encoder: Vanilla Transformers (Vaswani et al., 2017) and Multimodal Bottleneck Transformers (MBT (Nagrani et al., 2021)). The vanilla Transformer $g_{\text{av}}(\cdot)$ jointly encodes audio and video tokens as $(\mathbf{a}_{\text{um}}^{l+1} \parallel \mathbf{v}_{\text{um}}^{l+1}) = \text{Transformer}^l(\mathbf{a}_{\text{um}}^l \parallel \mathbf{v}_{\text{um}}^l)$, where “ \parallel ” means concatenation. The bottleneck variant tries to encourage the model to more selectively collate and condense relevant information in each modality by forcing information exchange between modalities to pass through a small number of learnable bottleneck features $\mathbf{b}^0 = [b_1 \dots b_4]$, $b_i \in \mathbb{R}^H$, as originally proposed in MBT for supervised audio-video learning. Precisely, $\mathbf{a}_{\text{um}}^{l+1} \parallel \mathbf{b}_a^{l+1} = g_{\text{av}}^l(\mathbf{a}_{\text{um}}^l \parallel \mathbf{b}^l)$ and $\mathbf{v}_{\text{um}}^{l+1} \parallel \mathbf{b}_v^{l+1} = g_{\text{av}}^l(\mathbf{v}_{\text{um}}^l \parallel \mathbf{b}^l)$, where $\mathbf{b}^{l+1} = (\mathbf{b}_a^{l+1} + \mathbf{b}_v^{l+1})/2$. In each variant, we stack L Transformer blocks to produce the audio-video jointly encoded output \mathbf{a}_{mm} and \mathbf{v}_{mm} .

We use standard Transformer blocks as the audio and video decoders. The encoded tokens from the fusion encoder are then projected and padded with trainable [MASK] tokens. After restoring the original order (time-frequency for audio tokens and space-time for video tokens), we add the decoder’s (fixed 2-D sinusoidal) positional embeddings and feed the restored sequence into the decoder $f_a^{-1}(\cdot)$ and $f_v^{-1}(\cdot)$. At the top of the decoder stack of each modality, we add a linear head to reconstruct the input spectrogram and pixels. Formally, the decoder output for spectrogram reconstruction is $\hat{\mathbf{a}} = f_a^{-1}(g_{\text{av}}(f_a(\mathbf{a}')))$ and the pixel reconstruction is $\hat{\mathbf{v}} = f_v^{-1}(g_{\text{av}}(f_v(\mathbf{v}')))$. For notation clarity, we omit the [MASK] tokens and linear projection head.

Let $\hat{\mathbf{a}}_i, i = 1 \dots n$ be the reconstruction of i -th masked spectrogram patch generated by the decoder’s reconstruction head. Similarly, $\hat{\mathbf{v}}_j, j = 1 \dots m$ for video patches. In masked audio-video reconstruction, MAViL is self-supervised by minimizing the reconstruction objective $\mathcal{L}_r^{\text{raw}}$ defined as:

$$\mathcal{L}_r^{\text{raw}} = \frac{1}{n} \sum_{i=1}^n (\hat{\mathbf{a}}_i - \mathbf{a}_i)^2 + \frac{1}{m} \sum_{j=1}^m (\hat{\mathbf{v}}_j - \mathbf{v}_j)^2. \quad (1)$$

3.2. Contrastive Audio-Video Learning with Masking

With the natural audio-visual alignment found in videos, we aim to learn from spatiotemporal correspondences within

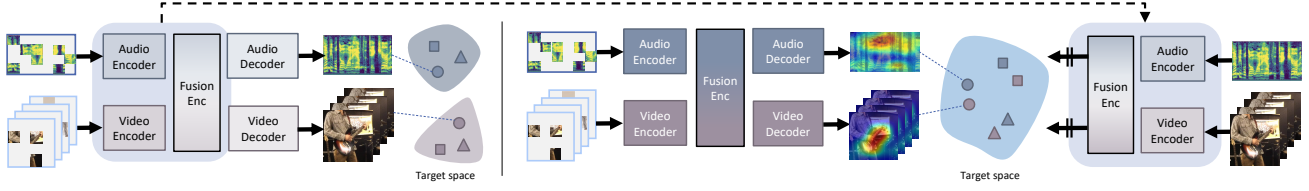


Figure 2. **Masked multimodal contextualized reconstruction** in the aligned multimodal latent space. Stage-1 (left): Training MAViL teacher with raw inputs as the targets. Stage-2 (right): Distilling to MAViL student with teacher’s multimodal contextualized features (complementary and aligned with masked autoencoding and contrastive learning after Stage-1) as the targets.

and across modalities in a self-supervised fashion. We use contrastive learning to enforce alignment among multiple “views” from the same training instance. The “views” to be aligned can be *within modality* observations of the instance itself or its semantic observations in *different modalities* (e.g., a video and its corresponding audio track). We use the InfoNCE (van den Oord et al., 2018) loss for contrastive learning. Let $\mathbf{x} = [\mathbf{x}_1 \dots \mathbf{x}_B]$, $\mathbf{y} = [\mathbf{y}_1 \dots \mathbf{y}_B]$; $\mathbf{x}_i, \mathbf{y}_j \in \mathbb{R}^H$ be the instance-level representations of audio/video in a size B sampled batch. The contrastive loss $\mathcal{L}_c(\mathbf{x}, \mathbf{y})$ is defined as:

$$\mathcal{L}_c(\mathbf{x}, \mathbf{y}) = -\frac{1}{B} \sum_{i=1}^B \log \frac{\exp(\mathbf{S}(\mathbf{x}_i, \mathbf{y}_i)/\tau)}{\sum_{j=1}^B \exp(\mathbf{S}(\mathbf{x}_i, \mathbf{y}_j)/\tau)}, \quad (2)$$

where $\mathbf{S}(\mathbf{x}_i, \mathbf{y}_j) = \frac{\mathbf{x}_i^T \mathbf{y}_j}{\|\mathbf{x}_i\| \|\mathbf{y}_j\|}$ is the cosine similarity between embeddings $\mathbf{x}_i, \mathbf{y}_j$ and τ is the softmax temperature. We design two types of contrastive objectives for self-supervised learning from audio-video pairs: 1) *inter-modal* contrastive learning $\mathcal{L}_c^{\text{inter}}$ and 2) *intra-modal* contrastive learning $\mathcal{L}_c^{\text{intra}}$.

Inter-modal contrastive learning promotes *cross-modal alignment* (intuitively, the audio and visual embeddings of a video should be close to each other). MAViL performs contrastive learning over *masked* instances for better computation efficiency and to jointly train with the masked reconstructing loss above. We first average embeddings from uni-modal encoders over the sequence length, namely, $\mathbf{a}_{\text{emb}} = \text{Avg}(\mathbf{a}_{\text{um}})$ and $\mathbf{v}_{\text{emb}} = \text{Avg}(\mathbf{v}_{\text{um}})$. The positive pairs are the video and audio clips from the same video, while all the other combinations of audio-video pairs are considered negatives. $\mathcal{L}_c^{\text{inter}}$ draws closer the representations of paired audio and video and meanwhile pushes away the mismatched ones. Minimizing it effectively learns an audio-video latent space where semantically similar instances in different views (e.g. paired audio-video) are close to each other and instances are distant if they are uncorrelated. We do *not* use the fusion output \mathbf{a}_{mm} and \mathbf{v}_{mm} for contrastive learning since the joint encoding layer provides a shortcut of cross-modal information exchange for every paired audio-video clip, resulting in sub-optimal performance.

Intra-modal contrastive learning promotes *within-modality alignment*, where the representations of different views, i.e., different masked samples of an audio (or video)

stream should be close to each other. For each modality, we sample a second random view containing 20% of tokens that are mutually exclusive from the first view. We then use encoded representations from these views as the positive pairs to contrast against other instance-level representations of the same modality in the training batch as negatives.

Formally, the inter- and intra-modal contrastive objectives in MAViL are defined as:

$$\begin{aligned} \mathcal{L}_c^{\text{inter}} &= \mathcal{L}_c(\mathbf{a}_{\text{emb}}, \mathbf{v}_{\text{emb}}), \\ \mathcal{L}_c^{\text{intra}} &= \frac{1}{2} [\mathcal{L}_c(\mathbf{a}_{\text{emb}}, \tilde{\mathbf{a}}_{\text{emb}}) + \mathcal{L}_c(\mathbf{v}_{\text{emb}}, \tilde{\mathbf{v}}_{\text{emb}})], \end{aligned} \quad (3)$$

where $\tilde{\mathbf{a}}_{\text{emb}}$ and $\tilde{\mathbf{v}}_{\text{emb}}$ represent the second view sampled from different time-frequency and space-time locations for audio and video modalities, respectively. Overall, MAViL is self-supervised by minimizing the following objective:

$$\mathcal{L}_{\text{MAViL}} = \mathcal{L}_r^{\text{raw}} + \alpha \mathcal{L}_c^{\text{inter}} + \beta \mathcal{L}_c^{\text{intra}}. \quad (4)$$

where α and β are the weights that balance loss functions.

3.3. Masked Multimodal Contextualized Reconstruction

To learn multimodal representations that capture joint audio-visual information, we go beyond reconstructing raw uni-modal (audio *or* video) inputs as in MAE and design a new pretext task that reconstructs multimodal contextualized representations in the *joint* latent space. To achieve this, we simply employ a 2-stage training framework illustrated in Fig. 2. In the 1st stage, we follow the training paradigm introduced in §3 to train a MAViL *teacher* model by reconstructing spectrograms and pixels. In the 2nd stage, we extend the training framework into a teacher-student framework. We freeze MAViL trained in the 1st stage and treat it as the teacher to generate contextualized multimodal features as reconstruction targets. These targets then guide the learning of the re-initialized *student* MAViL.

We forward complete-view audio and video to the audio, video, and fusion encoders of the frozen teacher network $\mathbf{a}^{\text{Teacher}} \parallel \mathbf{v}^{\text{Teacher}} = g_{\text{av}}^{\text{Teacher}}(f_{\text{a}}^{\text{Teacher}}(\mathbf{a}) \parallel f_{\text{v}}^{\text{Teacher}}(\mathbf{v}))$. Masked-view audio and video tokens are passed through student MAViL encoders and decoders for reconstruction (i.e., $\tilde{\mathbf{a}} = f_{\text{a}}^{-1}(g_{\text{av}}(f_{\text{a}}(\mathbf{a}')))$) as the audio feature prediction;

and $\tilde{\mathbf{v}} = f_v^{-1}(g_{av}(f_v(\mathbf{v}')))$ as the video feature prediction). The contextualized reconstruction objective is defined as:

$$\mathcal{L}_r^{\text{context}} = \frac{1}{n} \sum_{i=1}^n (\tilde{\mathbf{a}}_i - \mathbf{a}_i^{\text{Teacher}})^2 + \frac{1}{m} \sum_{j=1}^m (\tilde{\mathbf{v}}_j - \mathbf{v}_j^{\text{Teacher}})^2. \quad (5)$$

In the 2nd stage training, we jointly minimize the masked contextualized reconstruction objective and the contrastive objectives¹. The student MAViL’s objective is:

$$\mathcal{L}_{\text{MAViL}} = \mathcal{L}_r^{\text{context}} + \alpha \mathcal{L}_c^{\text{inter}} + \beta \mathcal{L}_c^{\text{intra}}. \quad (6)$$

Note that this objective contains pure latent targets. The teacher multimodal encoder encourages the student network to predict contextualized joint audiovisual representations with masked view inputs. We use the audio/video encoders in the final student model for fine-tuning downstream evaluation tasks.

4. Experiments

We conduct extensive evaluations including audio-video classification on AudioSet (Gemmeke et al., 2017) (AS-2M, AS-20K) and VGGSound (Chen et al., 2020); and audio-to-video retrieval on MSR-VTT (Xu et al., 2016); and YouCook (Zhou et al., 2018). We use AS-20K for model analysis and ablation studies.

4.1. Datasets

AudioSet (Gemmeke et al., 2017) (AS-2M, AS-20K) contains 2 million 10-second YouTube clips for audio event detection. 527 types of audio events are weakly annotated (Li et al., 2022; Hershey et al., 2017; 2021) for each clip, and multiple events can occur in one clip. The *full* training set has two subsets: A class-wise *balanced* (22K clips) and an *unbalanced* (2 million clips) set. The *eval* set has 20K clips. We downloaded around 1.97M unbalanced training, 20K balanced training, and 19K evaluation clips. For the AS-2M experiments, we use the union of unbalanced and balanced sets for pre-training and fine-tuning. For the AS-20K experiments, we use AS-2M for pre-training and the 20K balanced set for fine-tuning. We report the testing mAP on the 19K *eval* set used by AST (Gong et al., 2021).

VGGSound (Chen et al., 2020) contains around 200K video clips of 10-second length, annotated with 309 sound classes consisting of human actions, sound-emitting objects, and human-object interactions. The dataset is split into $\sim 183\text{K}$ train and $\sim 15\text{k}$ test samples. Unlike AudioSet, the audio event in each clip is guaranteed to be “visually present” in the video. We report top-1 classification accuracy.

¹We empirically observe that adding the raw autoencoding loss on pixel/spectrogram information as in the 1st stage of training does not provide any further gains.

4.2. Implementation Details

We use different temporal footprints for audio and video. For audio, following (Nagrani et al., 2021; Gong et al., 2021), we transform raw waveform (pre-processed into mono-channel under 16K sampling rate) into 128 Kaldi (Povey et al., 2011)-compatible Mel-frequency bands with a 25ms Hanning window that shifts every 10 ms. For a 10-second recording in AudioSet, the resulting spectrogram is of $1 \times 1024 \times 128$ dimension. We tokenize it as non-overlapped 16×16 patches (*i.e.*, kernel and stride are 16 for both time and frequency). The flattened audio token length N is 512. For video, MAViL takes 4-second clips (8 frames, 2 frames per second). The frame size is 224×224 . The spatial kernel and stride are 16×16 and the temporal kernel and stride is 2. The flattened audio token length N is 784.

We follow the main design choices of Audio-MAE (Huang et al., 2022a) and original MAE (He et al., 2022) for images. We use 12-layer Transformers (with 768-dimensions and 12 attention heads) as the encoders for each modality. The embedding dimension H is 768. The audio-video fusion encoder layer is a two-layer ($L=2$) (vanilla or MBT) Transformer on top of uni-modal encoders. Similarly, the audio and video decoders are 8-layer Transformers with an embedding dimension of 512 and 16 attention heads. The encoder and decoder in MAViL have 164M and 27M parameters, respectively. For balancing the losses in (4), we set $\alpha = 0.1$, $\tau_c^{\text{inter}} = 0.1$ and $\beta = 0.01$, $\tau_c^{\text{intra}} = 1.0$ to scale the gradients from three objectives into a comparable range to improve training stability.

For the audio branch, following (Huang et al., 2022a), we pre-train the audio Transformers from scratch. For the visual branch, we initialized the visual Transformer with the self-supervised MAE (He et al., 2022) pre-trained on ImageNet. MAViL operates under a fully self-supervised setup.

4.3. Experimental Setup

We pre-train MAViL on AudioSet-2M audio-video clips without using any labels. By default, we pre-train with 64 GPU with a 512 accumulated batch size and a 0.0002 learning rate (please refer to Appendix for detailed hyperparameters in all experiments). We pre-train for 20 epochs in each stage. Each stage takes ~ 20 hours.

We then evaluate the learned audio and video representations by fine-tuning on audio-video event classification tasks (AudioSet-20K, AudioSet-20M, VGGSound). We follow the setup in MAE to only keep the pre-trained audio and video encoders. We apply average pooling on top of the encoded tokens followed by a linear layer for classification. We use the standard fine-tuning pipeline in MAE and adopt hyperparameters and augmentation in prior audio-based and audio-video event classification works (Gong et al., 2021;

Huang et al., 2022a; Nagrani et al., 2021). Specifically, we use mixup (Zhang et al., 2018) and balanced sampling (Li et al., 2022) and fine-tuning masking (Huang et al., 2022a). We apply random time shifts and magnitude augmentation for audio and standard video augmentations in MAE for video (Feichtenhofer et al., 2022). We fine-tune the model under 3 scenarios: 1) audio-only, 2) video-only, and 3) audio+video. Empirically we observe a discrepancy in the convergence rate between audio and video. We circumvent this by applying a 50% learning rate reduction for the weights of the video encoder when performing audio+video fusion fine-tuning. Fine-tuning for 100 epochs on AS-2M takes ~ 10 hours. More details are in Appendix.

In the following, we first analyze MAViL on AS-20K (§4.4) and then present the main results compared to prior works in §4.5. The gray entries represent the default setup.

4.4. Model Analysis

Masked Audio-Video Learning. We start by examining the masking ratio, the key hyperparameter in MAE. We report the classification accuracy in AS-20K fine-tuning (after AS-2M pre-training) for both audio and video encoders. We use the same masking ratio for both audio and video and ablate different values in Table 1. The results suggest that 80% masking yields the best performance (and works slightly better than 70% or 90%). This is similar to the optimal values of 80% in Audio-MAE (Huang et al., 2022a), 90% in Video-MAE (Feichtenhofer et al., 2022), encoding only non-masked tokens significantly reduces the sequence length and therefore computation (which scales quadratically to the length in self-attention layers of Transformers).

Ratio	50%	60%	70%	80%	90%
Audio	35.3	36.5	36.7	36.8	36.8
Video	17.0	17.3	17.5	17.7	17.5

Table 1. **Masking Ratio.** Performance is measured as mAP in AS-20K for individual fine-tuning as Audio or Video classification.

We next investigate the improvements by learning with complementary multimodal information in masked autoencoding. We ablate either using a vanilla Transformer stack or MBT to fuse multimodal information for reconstructing raw input. Table 2 summarizes the accuracy on AS-20K for using either 2 or 4 layers of fusion encoder. The first column (None) reports the baselines without the joint audio-video encoder layer. MAE and video-MAE baselines without the fusion audio-video encoder layer. Using fusion leads to +0.4 mAP gain for audio and video. Although MBT layers achieve better results, the difference is not significant over using vanilla Transformers for masked audio-video learning. Two MBT⁽²⁾ Transformer blocks are sufficient and perform as well as four MBT⁽⁴⁾ blocks. We choose to use vanilla Transformers by default for simplicity.

Fusion Enc.	None	Vanilla ⁽²⁾	Vanilla ⁽⁴⁾	MBT ⁽²⁾	MBT ⁽⁴⁾
Audio	36.4	36.8	36.7	36.9	36.8
Video	17.4	17.8	17.6	17.8	17.7

Table 2. **Fusion Encoder:** Transformer type^(# layers). The “None” are the uni-modal MAE baselines (Audio-MAE and Video-MAE).

Contrastive Audio-Video Learning with MAE. Next, we investigate improvements when contrastive learning is used in conjunction with MAE. We employ an intra-contrastive loss on only 20% of visible patches in each modality. As shown in Table 3, our contrastive losses are shown to be important for learning audio-video representations. Both inter-modal and intra-modal contrastive learning improve the results, and combining them yields the best performance. Note that while audio and video are used jointly in pre-training, the fine-tuning is done with uni-modal encoders. Therefore the improvements for audio and video classification demonstrate that learning from both modalities can improve an individual modality.

Contrastive objs.	None	inter	intra	inter+intra
Audio	36.8	38.4	38.1	39.0
Video	17.8	21.0	19.8	22.2

Table 3. **Masked Contrastive Audio-Video Learning.**

We also experimented with alternative pooling functions to represent each instance in contrastive learning. Empirically, we observe a simple average pooling over uni-modal encoder output (*i.e.*, $\mathbf{a}_{\text{emb}} = \text{Avg}(\mathbf{a}_{\text{um}})$ for visible audio tokens, and similar for video) yields the best result, compared to using the [CLS] token (-0.3 mAP) or adding additional MLP layers (-0.3 mAP).

Multimodal Contextualized Reconstruction. As illustrated in Fig. 2, MAViL employs a two-stage training. In the 1st stage, we train a model to reconstruct raw inputs with masked and contrastive audio-video learning analyzed in the previous experiments. In the 2nd stage, we re-initialize the student MAViL model and train it to reconstruct the contextualized features generated by the frozen teacher from the 1st stage. We compare reconstruction targets in Table 4.

Target	Raw Inputs	A/V-MAE	MAViL-Uni	MAViL-Fusion
Audio	39.0	39.5	40.0	40.7
Video	22.2	23.1	23.8	24.1

Table 4. **Reconstruction Target** for the 2nd stage MAViL. Raw: spectrogram/pixel (column 1). Contextualized: A-MAE/V-MAE (uni-modal output, column 2); MAViL-Uni (uni-modal output, column 3); MAViL-Fusion (multimodal fusion output, column 4).

Our multimodal contextualized reconstruction predicts pre-trained MAViL teacher’s multimodal fusion encoder output (*i.e.*, $g_{\text{av}}^{\text{Teacher}}(f_{\text{a}}^{\text{Teacher}}(\mathbf{a}) \| f_{\text{v}}^{\text{Teacher}}(\mathbf{v}))$, MAViL-Fusion).

First we compare it with raw input reconstruction and single modal contextualized reconstruction (*i.e.*, predicting separately pre-trained (uni-modal) Audio-MAE and Video-MAE teachers' encoder output). The results show that predicting MAViL teacher's fusion encoder output outperforms predicting uni-modal MAEs output or raw spectrogram/pixels (identical to one-staged MAViL).

Next we compare with reconstructing (uni-modal) MAViL-Uni Teacher features (*i.e.*, $f_a^{\text{Teacher}}(\mathbf{a})$ and $f_v^{\text{Teacher}}(\mathbf{v})$ which is before the fusion encoder in Fig. 2). The results imply that stronger audio-video representations (+0.7 for audio mAP) can be learned by masked prediction of contextualized and synchronized multimodal features, even though they are generated by a pre-trained MAViL teacher without external data or model. The gain with multimodal contextualized reconstruction is (+1.7 audio and +1.9 video mAP).

Additional Ablations. Additional ablations are summarized in Table 5. We draw the following observations:

- (a) Larger data size is critical for self-supervised learning (Tab. 5a ablates using 10%, 50% or 100% of AS-2M for pre-training of MAViL).
- (b) Longer pre-training is beneficial and 20 epochs are sufficient (Table 5b) for good performance.
- (c) Tuning contrastive loss weights is helpful (Table 5c).
- (d) ImageNet pre-training is useful for the video classification stream (Table 5d). Initializing from an ImageNet fine-tuned model that uses labels (IN-SL) is beneficial yet we avoid using it to keep MAViL fully self-supervised.
- e) Increasing the encoder sizes (ViT-S/B/L) improves mAP (Table 5e); we use ViT-B for efficiency as default.

AS-2M	10%	50%	100%	epoch	10	15	20	25
Audio	33.1	39.2	40.7	Audio	39.1	40.1	40.7	40.7
Video	19.3	22.5	24.1	Video	20.4	22.5	24.1	24.2

(a) Dataset size

(b) pre-training epoch

α	0.3	0.1	0.05	Init.	Scratch	IN-SSL	IN-SL
Audio	40.5	40.7	40.2	Audio	40.5	40.7	40.7
Video	19.6	24.1	23.6	Video	22.6	24.1	24.7

(c) Contrastive weight

(d) Visual backbone initialization

Backbone	ViT-S	ViT-B	ViT-L
Audio	36.2	40.7	41.8
Video	20.5	24.1	25.2

(e) Model Size

Table 5. Additional ablations on AS-20K.

In summary, MAViL boost the uni-modal MAE accuracy from 36.4→40.7 mAP for audio and 17.4→24.1 mAP for video encoders, clearly showing that learning from audio and video can improve each modality individually.

Method	PT	AS-20K			AS-2M		
		A	V	A+V	A	V	A+V
<i>Audio-only Models</i>							
PANNs (Kong et al., 2020)	-	27.8	-	-	43.9	-	-
AST (Gong et al., 2021)	SL	34.7	-	-	45.9	-	-
HTS-AT (Chen et al., 2022)	SL	-	-	-	47.1	-	-
PaSST (Koutini et al., 2021)	SL	-	-	-	47.1	-	-
Data2vec (Baeviski et al., 2022)	SSL	34.5	-	-	-	-	-
SSAST (Gong et al., 2022a)	SSL	31.0	-	-	-	-	-
MAE-AST (Baade et al., 2022)	SSL	30.6	-	-	-	-	-
Aud-MAE(Huang et al., 2022a)	SSL	37.0	-	-	47.3	-	-
<i>Audio-Video Models</i>							
G-Blend (Wang et al., 2020)	-	29.1	22.1	37.8	32.4	18.8	41.8
Perceiver (Jaegle et al., 2021)	-	-	-	-	38.4	25.8	44.2
CAV-MAE [†] (Gong et al., 2022b)	SSL	37.7	19.8	42.0	46.6	26.2	51.5
Attn AV (Fayek & Kumar, 2020)	SL	-	-	-	38.4	25.7	46.2
MBT [*] (Nagrani et al., 2021)	SL	31.3	<u>27.7</u>	43.9	44.3	<u>32.3</u>	52.1
<i>Our Audio-Video Models</i>							
MAViL-Stage1	SSL	39.0	22.2	42.5	47.4	28.1	51.8
MAViL	SSL	40.7	24.1	44.3	48.4	30.2	53.1

Table 6. Comparison to prior works on AudioSet (AS). mAP[†] is reported for audio (A), video (V) and audio+video (A+V) classification. MAViL uses ViT-B encoders for each modality. Models are pre-trained on AS-2M and fine-tuned on either AS-20K or AS-2M. PT: pre-training type; SL: (ImageNet) supervised learning; SSL: self-supervised learning; [†]: concurrent work. ^{*}We de-emphasize the model with non-standard training/testing split. We underline the best model and bold the best self-supervised model. Table 7-9 follow the same notations.

4.5. Main Results

We compare MAViL with other previous models on the standard benchmarks. We denote the first-stage MAViL (trained with Eq. 4 as MAViL-Stage1. The full model MAViL is the second-stage student trained with Eq. 6.

Audio-Video Event Classification. Table 6 summarizes the performance comparison on AudioSet (AS). We report accuracy for fine-tuning the audio (A), video (V) or audio-video encoders (A+V). Our MAViL sets new state-of-the-art audio-only, audio+video classification accuracy on both the unbalanced AS-2M and balanced AS-20K. Compared to all the self-supervised audio-only or audio-video models under AudioSet, MAViL outperforms them by a large margin. MAViL outperforms the concurrent CAV-MAE (Gong et al., 2022b). We attribute this to our multimodal contextualized reconstruction and improved contrastive learning with both inter-modal and intra-modal contrast. MAViL also outperforms data2vec (Baeviski et al., 2022), demonstrating the superiority of using aligned multimodal contexts (Eq. 5) as the reconstruction targets over uni-modal contexts.

For the first time, our fully self-supervised MAViL outperforms supervised audio-video models (*e.g.*, MBT (Nagrani et al., 2021)) on audio and audio+video classification tasks. However, compared to MBT, the fully self-supervised

Method	PT	A	V	A+V
CAV-MAE [†] (Gong et al., 2022b)	SSL	59.5	47.0	65.5
AV-SlowFast (Xiao et al., 2020)	SL	50.1	-	-
VGGSound (Chen et al., 2020)	SL	48.8	-	-
MBT (Nagrani et al., 2021)	SL	52.3	51.2	64.1
MAViL-Stage1	SSL	59.9	48.3	63.8
MAViL	SSL	60.8	50.9	67.1

Table 7. VGGSound results (Accuracy \uparrow).

Method	PT	ESC-50	SPC-1
AST (Gong et al., 2021)	SL	88.7	95.5
SS-AST (Gong et al., 2022a)	SSL	88.8	96.0
MAE-AST (Baade et al., 2022)	SSL	90.0	95.8
Aud-MAE (Huang et al., 2022a)	SSL	94.1	96.9
MAViL	SSL	94.3	97.4

Table 8. Comparison on audio-only tasks (Accuracy \uparrow).

trained video backbone still needs to catch up in performance, likely due to the fact that the visual part in AudioSet is noisy and is not necessarily relevant to the audio events (Mohamed et al., 2022). Such dataset bias could make the visual pre-training sub-optimal. This is a constraint of pre-training on AudioSet.

Notably, comparing MAViL-Stage1 and (teacher-guided) MAViL (both are with (inter-/intra-)modal contrastive learning), there is consistent and significant improvement of the later with multimodal contextualized reconstruction. This implies that multimodal contextualized reconstruction is complementary to contrastive learning, on top of the base-lines using autoencoding of raw inputs (*cf.* Table 4).

The comparison on VGGSound is shown in Table 7. MAViL again sets a new state-of-the-art for audio-only and audio+video classification tasks where it greatly outperforms MBT and the concurrent CAV-MAE. In this out-of-pre-training-domain task, we observe similar improvements for multimodal contextualized reconstruction shown by the gain of MAViL for audio-visual classification (A+V) over the 1st stage (67.1% vs. 63.8% accuracy) of training.

Transfer to Audio/Speech-only tasks. To test the generalizability of the learned audio representations, we further evaluate them by transferring AS-pre-trained MAViL to other out-of-domain speech-only or audio-only tasks. We conduct experiments on the Environmental Sound Classification (ESC-50) (Piczak, 2015) and Speech Commands (SPC-V1) (Warden, 2018) datasets. We fine-tune only the audio branch of AudioSet pre-trained MAViL. The results are summarized in Table 8. MAViL outperforms all recent supervised and self-supervised models and achieves a new state-of-the-art. MAViL demonstrates desirable transferability from audio-video self-supervised pre-training to audio-only downstream tasks.

Method	PT data	MSR-VTT	YouCook
AVLNet (Rouditchenko et al., 2021)	HT100M	20.1	30.7
TVLT (Tang et al., 2022)	HT100M	22.6	31.8
MAViL	AS-2M	22.2	31.3
MAViL	HT-100M	23.5	33.0

Table 9. Comparison on audio-to-video retrieval tasks in VTT and YouCook. (Recall@1 \uparrow)

Audio-to-Video Retrieval. Beyond classification tasks, MAViL learns synchronized audio-video representations which are feasible for textless cross-modal retrieval. To evaluate the quality of the learned representations, we conduct audio-to-video retrieval experiments on MSR-VTT and YouCook. In this task, a model encodes the audio track of a video as the query and performs a search over the testing video collection by measuring and ranking the similarity between the query embedding and the video embeddings of testing videos. We fine-tune MAViL with the audio-video pairs in the training sets and report the retrieval performance under the standard recall@1 metric on the testing sets.

Following AVLNet (Rouditchenko et al., 2021) and TVLT (Tang et al., 2022), we also investigate an additional setup to pre-train on HowTo100M (Miech et al., 2019), a 1.3 million instructional video collection, instead of pre-training on AudioSet. Note that there are clear domain gaps between pre-training datasets (AudioSet or HowTo100M) and the target datasets (MSR-VTT or YouCook). As shown in Table 9, our model outperforms supervised pre-trained models (AVLNet (Rouditchenko et al., 2021) and self-supervised pre-trained model (TVLT (Tang et al., 2022) and set new SOTA performance on this task.

Qualitative Visualizations of MAViL-stage1 audio and video decoders can be found in the Appendix.

5. Conclusion

We have presented MAViL, a self-supervised audio-video representation learning framework where masked autoencoding meets contrastive learning. MAViL includes a set of three objectives for learning complementary and aligned audio-video representations. First, we use multimodal masked autoencoding to reconstruct raw inputs in each modality with an encoder-fusion-decoder architecture. Second, we apply contrastive learning to associate masked audio-video embeddings, both within and across modalities. Third, we show that the trained model can serve as a multimodal teacher, to guide new MAViL students in learning stronger audio-video representations. By aligning and reconstructing contextualized audio-video representations, the fully self-supervised MAViL sets a new state-of-the-art compared to recent work in seven audio and audio-video classification and retrieval tasks outperforming also models with external supervision.

Appendix

The Appendix is organized as follows: In §A, we first demonstrate qualitative audio and video reconstruction results. In §B, we provide the complete experimental details and hyper-parameters for pre-training and fine-tuning on each dataset.

A. Audio-Video Reconstructions by MAViL-stage1 Decoders

For visualization, we employ MAViL with ViT-B as the audio and video backbone. We train it with 80% masking ratio on the AudioSet-2M (AS-2M) training set with raw spectrograms and video frames as its reconstruction targets (Eq. 4). We then visualize the reconstruction by the MAViL decoder with 70% input tokens masked to its encoder on AudioSet eval set. The results are shown in Fig. 3.

As can be observed, MAViL successfully reconstructs both the audio spectrogram and video frames of a video clip from their extremely corrupted versions. For videos, the generated reconstructions are of high fidelity and maintain spatial and temporal consistency of visual objects across a variety of input domains, scenes, and lighting conditions. For audio reconstruction, MAViL respects the positions and arrangements of time-frequency components in the spectrogram, which are crucial for humans to understand and perceive sound. The audio and video are consistent and well-aligned in time.

B. Experimental Details & Hyperparameters

In this section, we provide additional experimental details for data preprocessing, implementation, pre-training, fine-tuning, and inference. The hyperparameters are summarized in Table 10. The code and pre-trained models to reproduce the results will be available soon.

Data Preprocessing. We downloaded and preprocessed 2.01 million AudioSet videos (with both video and audio track) and 198K VGGSound videos. We resize the video track with 360p (keep the aspect ratio and longer dimension is 260 and re-sample audio into 16,000 sampling rate. We use different temporal footprints for audio and video.

For the audio part, following (Nagrani et al., 2021; Gong et al., 2021), we transform raw waveform (pre-processed into mono-channel under 16K sampling rate) into 128 Kaldi (Povey et al., 2011)-compatible Mel-frequency bands with a 25ms Hanning window that shifts every 10 ms. We normalize the spectrogram with the mean and variance calculated on the AudioSet training set. For a 10-second recording in AudioSet, the resulting (1-channel) spectrogram is of $1 \times 1024 \times 128$ dimension.

For the video part, we use 4-second clips (8 frames under 2 frames per second (fps)). The frame size is 224×224 with random horizontal flip (probability is 0.5) and multi-scale random crop (scale=(0.2, 1.0)) as data augmentations in pre-training. We apply no augmentation in the testing/inference phase. For a 10-second video clip in AudioSet, we randomly sample the starting point and take the consecutive 4 seconds (cyclically loop to the beginning if it is shorter than 4 seconds) to construct the 4-second video clip input. The resulting (3-channel) video clip is of $8 \times 3 \times 224 \times 224$ dimension.

Implementation. We follow the main design choices of Audio-MAE (Huang et al., 2022a) and original MAE (He et al., 2022) for images. We use separated 12-layer Transformers (with 768-dimensions and 12 attention heads) as the encoders for each modality. The embedding dimension H is 768 in all Transformers (ViT-B as default).

The patch embedding layers are also separated. For each $1 \times 1024 \times 128$ input spectrogram of a 10-second audio, we tokenize it into non-overlapping 16×16 spectrogram patches with an audio patch embedding layer. The kernel and stride in the audio patch embedding is 16 for both time and frequency. There are 64×8 spectrogram patches/tokens. The length N of flattened audio token sequence is 512. Each audio token is a 768-dimensional vector. After appending the [CLS] token, adding positional embedding, and applying 80% of masking, the final input audio token sequence $\mathbf{a}' \in \mathbb{R}^{103 \times 768}$. For each $8 \times 3 \times 224 \times 224$ video clip (4-second long), we tokenize it into non-overlapped $2 \times 16 \times 16$ cells/patches with a video patch embedding layer. The spatial kernel and stride is 16×16 and the temporal kernel and stride is 2, resulting in $4 \times 14 \times 14$ video patches/tokens. The length M of flattened video token sequence is 784. Each video token is a 768-dimensional vector. After appending the [CLS] token, adding positional embedding, and applying 80% of masking, the final input audio token sequence $\mathbf{v}' \in \mathbb{R}^{158 \times 768}$.

We also investigated alternative design choices such as sharing audio-video encoder weights with separated inputs or concatenated as in Multi-MAE (Bachmann et al., 2022). However these alternative architectures delivers worse performance compare to the proposed architecture (separated encoder with separated inputs).

The audio-video fusion encoder layer is a two-layer ($L=2$) (vanilla or MBT (Nagrani et al., 2021)) Transformer on top of uni-modal encoders. In the MBT setup, we append additional 4 trainable MBT tokens for each modality after the uni-modal encoder output. The audio and video decoders are 8-layer Transformers with an embedding dimension of 512 and 16 attention heads. The encoder and decoder in MAViL have 164M and 27M parameters, respectively.

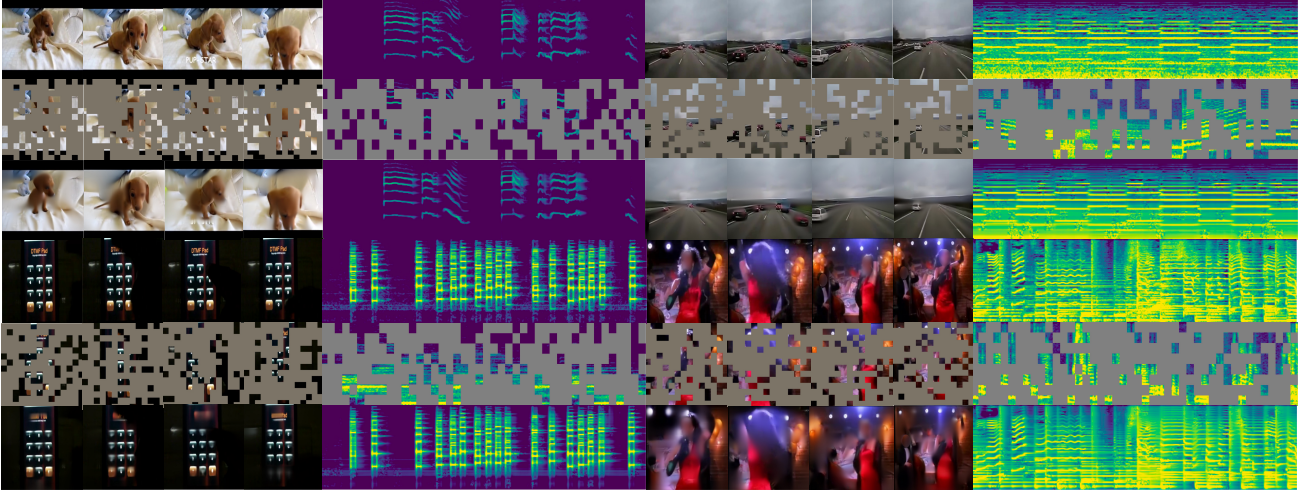


Figure 3. **Video clip and spectrogram reconstruction on the AudioSet eval set.** We sample 4 paired (video, audio spectrogram) as follows: Top left: a puppy video; Top right: a recording from an ambulance’s dash camera; Bottom left: a person dialing a phone in a dark room; Bottom right: a singer dancing. Input masking ratio: 70%. In each 3-row group, we show the original video and its audio (spectrogram) (top), masked input (middle), and MAViL output (bottom). The spectrogram shape is 1024×128 ; patch size is 16×16 . Each spectrogram has $64 \times 8 = 512$ patches with 154 (70% masked) patches being visible to MAViL. The 8-frame video clip size is $8 \times 3 \times 224 \times 224$; patch size is 16×16 . Each video has $4 \times 196 = 784$ patches after patch embedding (temporal kernel/stride=2) with 235 (70% masked) patches being visible to MAViL.

The softmax temperature in NCE (Eq. 2) is set to $\tau_c^{\text{inter}} = 0.1$ (more tolerant) for inter-modal contrastive learning and $\tau_c^{\text{intra}} = 1.0$ (stricter) for intra-modal contrastive learning. For balancing the losses in (4), we set $\alpha = 0.1$ and $\beta = 0.01$ to scale the gradients from three objectives into a comparable range to improve training stability.

Pre-training. We pre-train MAViL on the union of unbalanced and balanced training sets of AS-2M. By default, we pre-train with 64 A100 GPU with a 512 accumulated batch size and a 0.0002 base learning rate. We pre-train for 20 epochs in each stage. Each stage takes ~ 20 hours. Note that the effective learning rate (lr_{eff}) depends on the base learning rate (lr_{base}) and the batch size. Precisely, $lr_{\text{eff}} = lr_{\text{base}} * \frac{\text{batch size}}{256}$. We also experimented using strong data augmentations (e.g., mixup (Zhang et al., 2018), SpecAug (Zhang et al., 2018), and CutMix (Yun et al., 2019)) for audio and video pre-training but found the resulting performance similar or worse. Therefore we discard these strong data augmentations for audio and video in the pre-training phase by default.

Besides the proposed two-stage training framework, we also experimented with a one-stage variant that exploits the exponential move average (EMA) of MAViL (with raw input as the targets) as the teacher (similar to data2vec (Baevski et al., 2022)) to generate contextualized targets to be reconstructed by a separated decoder head in each modality. This setup results in less stable training behavior in the audio-video scenario of our concern. This is likely due to asynchronous convergence behavior in each modality,

which is also observed in (Wang et al., 2020). The final one-stage performance with EMA is worse than the proposed two-stage training.

Fine-tuning. For fine-tuning on audio-video (e.g., AudioSet-20K, AudioSet-20M, VGGSound) and audio/speech-only (e.g. ESC, SPC) classification tasks, we follow the setup in MAE to only keep the pre-trained audio and video encoders (both are ViT-B). We average pool the encoded tokens and apply a linear layer for classification. We use the standard fine-tuning pipeline in MAE and adopt hyperparameters and augmentation in prior audio-based and audio-video event classification works (Gong et al., 2021; Huang et al., 2022a; Nagrani et al., 2021). Specifically, we use mixup (Zhang et al., 2018) and balanced sampling (Li et al., 2022) and fine-tuning masking (Huang et al., 2022a) (a 20% random masking rate for time and frequency in audio spectrograms; 20% for space and time in video clips). We apply random time shifts and magnitude augmentation for audio and apply standard video augmentations such as random horizontal flip and random multi-scale cropping for video (Feichtenhofer et al., 2022).

To perform importance sampling that balance the fine-tuning scheme on the unbalanced AS-2M (and VGGSound), we apply a distributed weighted sampler as prior works (Li et al., 2022; Gong et al., 2021; Chen et al., 2022; Koutini et al., 2021). We set the probability of sampling a sample proportional to the inverse frequency of its labels, where the label frequency is estimated over the training set. Specifically, for a instance i in a dataset \mathcal{D} with a label pool \mathcal{C} ,

Configuration	Pre-training	Fine-tuning				
	AS-2M PT	AS-2M	AS-20K	VGGSound	ESC	SPC
Optimizer	AdamW (Loshchilov & Hutter, 2019)					
Optimizer momentum	$\beta_1 = 0.9, \beta_2 = 0.95$					
Weight decay	0.00001					
Base learning rate	0.0002	0.0002 [†]	0.001	0.0002	0.001	0.001
Learning rate schedule	half-cycle cosine decay (Loshchilov & Hutter, 2017)					
Minimum learning rate	0.000001					
Gradient clipping	None					
Warm-up epochs	4	20	4	4	4	1
Epochs	20	100	60	60	60	10
Batch size	512	512	64	256	64	256
GPUs	64	64	8	32	4	4
Weighted sampling	False	True	False	True	False	False*
Weighted sampling size	-	200,000	-	200,000	-	-
Augmentation	R	R	R	R+N	R	R+N
SpecAug (Park et al., 2019a) (time/frequency)	-	192/48	192/48	192/48	96/24	48/48
Drop path (Larsson et al., 2017)	0.0	0.1	0.1	0.1	0.1	0.1
Mixup (Zhang et al., 2018)	0.0	0.5	0.5	0.5	0.0	0.5
Multilabel	n/a	True	True	False	False	False
Loss Function	MSE	BCE	BCE	BCE	CE	BCE
Dataset Mean for Normalization	-4.268	-4.268	-4.268	-5.189	-6.627	-6.702
Dataset Std for Normalization	4.569	4.569	4.569	3.260	5.359	5.448

Table 10. Pre-training (PT) and Fine-tuning (FT) hyperparameters. For augmentation, R: sampling random starting points with cyclic rolling in time; N: adding random noise (signal-to-noise ratio (SNR): 20dB) to spectrograms. For loss functions, BCE: binary cross entropy loss (for multi-label datasets or when using mixup); CE: cross-entropy loss, MSE: mean square error loss. *: We repeat and balance each class to 50% of the size of the unknown class. †: For ViT-S, We use a learning rate of 0.0005 on AS-2M FT and 0.002 on AS-20K FT as we find larger learning rates work better for ViT-S encoder in the ablation study.

its sampling weight is proportional to $\sum_{c_i \in C} w_c$, where $w_c = \frac{1000}{\sum_{i \in D} c_i + \epsilon}$ and $\epsilon = 0.01$ is set to avoid underflow in majority classes. In each fine-tuning epoch on AS-2M, we sample 200K instances ($\sim 10\%$ of AS-2M) with replacement. We fine-tune for 100 epochs, which aggregate to ~ 10 full epochs of AS-2M and takes ~ 10 hours.

In the case where the task concerns multi-label classification (e.g. AS-2M) or the mixup augmentation is enabled (e.g., AS-20K and VGGSound), we use binary cross-entropy loss (BCE) as the fine-tuning objective without label smoothing (Müller et al., 2019) otherwise we use cross-entropy (CE) (e.g. the experiments on ESC).

We fine-tune the model under 3 scenarios: 1) audio-only, 2) video-only, and 3) audio+video. In audio-only and video-only scenario, we fine-tune the audio or video encoder in the (second-stage) MAViL. We apply the hyperparameter setups specified in Table 10. In the audio+video setup, we append a 3-layer vanilla Transformer on top of the audio and video encoder in the (second-stage) MAViL and fine-tune it with audio and video input. Empirically we observe a discrepancy in convergence rate between audio and video. We circumvent this by applying a 50% learning rate reduction for the weights of the video encoder when performing audio+video fusion fine-tuning.

Inference. After finetuning, we simply pick the last checkpoint for inference. For video and audio+video tasks, we follow the common practice in video action recognition (Feichtenhofer et al., 2019; Fan et al., 2021; Li et al., 2021) to uniformly sample 10 4-second video clips over the time domain of a video; and we feed forward the sampled 10 video clips to generate the prediction for each of them. Note that for audio+video classification, the audio input is the same 10-sec audio recording.

We average the 10 predictions as the instance-level prediction and report the classification performance in Table 6-7. Note that these are still single-modal results instead of ensembling multiple models. Table 11 compares the 1-clip prediction and 10-clip prediction results (mAPs on AS-2M).

# Clips (AS-2M)	1	10
Audio	48.4	48.4
Video	29.0	30.2
Audio+Video	52.6	53.1

Table 11. Number of video clips in the inference time.

References

- Aleksic, P. S. and Katsaggelos, A. K. Audio-visual biometrics. *Proceedings of the IEEE*, 94(11):2025–2044, 2006.
- Arandjelovic, R. and Zisserman, A. Look, listen and learn. In *ICCV*, 2017.
- Arandjelovic, R. and Zisserman, A. Objects that sound. In *ECCV*, 2018.
- Aytar, Y., Vondrick, C., and Torralba, A. Soundnet: Learning sound representations from unlabeled video. In *NeurIPS*, 2016.
- Baade, A., Peng, P., and Harwath, D. MAE-AST: Masked autoencoding audio spectrogram transformer. In *Interspeech*, 2022.
- Bachmann, R., Mizrahi, D., Atanov, A., and Zamir, A. MultiMAE: Multi-modal multi-task masked autoencoders. *arXiv preprint arXiv:2204.01678*, 2022.
- Baevski, A., Hsu, W.-N., Xu, Q., Babu, A., Gu, J., and Auli, M. Data2vec: A general framework for self-supervised learning in speech, vision and language. In *ICML*, 2022.
- Bao, H., Dong, L., and Wei, F. BEiT: BERT pre-training of image transformers. In *ICLR*, 2021.
- Caron, M., Touvron, H., Misra, I., Jégou, H., Mairal, J., Bojanowski, P., and Joulin, A. Emerging properties in self-supervised vision transformers. In *ICCV*, 2021.
- Chen, H., Xie, W., Vedaldi, A., and Zisserman, A. VGGSound: A large-scale audio-visual dataset. In *ICASSP*, 2020.
- Chen, K., Du, X., Zhu, B., Ma, Z., Berg-Kirkpatrick, T., and Dubnov, S. HTS-AT: A hierarchical token-semantic audio transformer for sound classification and detection. In *ICASSP*, 2022.
- Chen, T. and Rao, R. R. Audio-visual integration in multimodal communication. *Proceedings of the IEEE*, 86(5):837–852, 1998.
- Cho, J. H. and Hariharan, B. On the efficacy of knowledge distillation. In *ICCV*, 2019.
- Chrupała, G. Visually grounded models of spoken language: A survey of datasets, architectures and evaluation techniques. *Journal of Artificial Intelligence Research*, 73:673–707, 2022.
- Dalal, N. and Triggs, B. Histograms of oriented gradients for human detection. In *2005 IEEE Computer Society Conference on Computer Vision and Pattern Recognition (CVPR 2005), 20-26 June 2005, San Diego, CA, USA*, pp. 886–893. IEEE Computer Society, 2005. doi: 10.1109/CVPR.2005.177. URL <https://doi.org/10.1109/CVPR.2005.177>.
- Devlin, J., Chang, M., Lee, K., and Toutanova, K. BERT: pre-training of deep bidirectional transformers for language understanding. In *NAACL-HLT*, 2019.
- Ephrat, A., Mosseri, I., Lang, O., Dekel, T., Wilson, K., Hassidim, A., Freeman, W. T., and Rubinstein, M. Looking to listen at the cocktail party: a speaker-independent audio-visual model for speech separation. *ACM Transactions on Graphics (TOG)*, 37(4):1–11, 2018.
- Fan, H., Xiong, B., Mangalam, K., Li, Y., Yan, Z., Malik, J., and Feichtenhofer, C. Multiscale vision transformers. In *ICCV*, 2021.
- Fayek, H. M. and Kumar, A. Large scale audiovisual learning of sounds with weakly labeled data. In *IJCAI*, 2020.
- Feichtenhofer, C., Fan, H., Malik, J., and He, K. Slowfast networks for video recognition. In *ICCV*, 2019.
- Feichtenhofer, C., Fan, H., Li, Y., and He, K. Masked autoencoders as spatiotemporal learners. In *NeurIPS*, 2022.
- Gemmeke, J. F., Ellis, D. P., Freedman, D., Jansen, A., Lawrence, W., Moore, R. C., Plakal, M., and Ritter, M. Audio set: An ontology and human-labeled dataset for audio events. In *ICASSP*, 2017.
- Gong, Y., Chung, Y.-A., and Glass, J. AST: Audio Spectrogram Transformer. In *Interspeech*, 2021.
- Gong, Y., Lai, C.-I., Chung, Y.-A., and Glass, J. R. SSAST: Self-Supervised Audio Spectrogram Transformer. In *AAAI*, 2022a.
- Gong, Y., Rouditchenko, A., Liu, A. H., Harwath, D., Karlinsky, L., Kuehne, H., and Glass, J. Contrastive audio-visual masked autoencoder. *arXiv preprint arXiv:2210.07839*, 2022b.
- Grill, J.-B., Strub, F., Altché, F., Tallec, C., Richemond, P. H., Buchatskaya, E., Doersch, C., Pires, B. A., Guo, Z. D., Azar, M. G., Piot, B., Kavukcuoglu, K., Munos, R., and Valko, M. Bootstrap your own latent: A new approach to self-supervised learning. In *NeurIPS*, 2020.
- Gutmann, M. and Hyvärinen, A. Noise-contrastive estimation: A new estimation principle for unnormalized statistical models. In Teh, Y. W. and Titterton, D. M. (eds.), *Proceedings of the Thirteenth International Conference on Artificial Intelligence and Statistics, AISTATS 2010, Chia Laguna Resort, Sardinia, Italy, May 13-15, 2010*, volume 9 of *JMLR Proceedings*, pp. 297–304. JMLR.org, 2010. URL <http://proceedings.mlr.press/v9/gutmann10a.html>.
- Harwath, D., Recasens, A., Surís, D., Chuang, G., Torralba, A., and Glass, J. Jointly discovering visual objects and spoken words from raw sensory input. In *ECCV*, 2018.
- He, K., Fan, H., Wu, Y., Xie, S., and Girshick, R. Momentum contrast for unsupervised visual representation learning. In *CVPR*, 2020.
- He, K., Chen, X., Xie, S., Li, Y., Dollár, P., and Girshick, R. Masked autoencoders are scalable vision learners. In *CVPR*, 2022.
- Hershey, S., Chaudhuri, S., Ellis, D. P. W., Gemmeke, J. F., Jansen, A., Moore, C., Plakal, M., Platt, D., Saurous, R. A., Seybold, B., Slaney, M., Weiss, R., and Wilson, K. CNN architectures for large-scale audio classification. In *ICASSP*, 2017. URL <https://arxiv.org/abs/1609.09430>.
- Hershey, S., Ellis, D. P., Fonseca, E., Jansen, A., Liu, C., Moore, R. C., and Plakal, M. The benefit of temporally-strong labels in audio event classification. In *ICASSP*, 2021.
- Hinton, G., Vinyals, O., and Dean, J. Distilling the knowledge in a neural network. *NeurIPS Deep Learning and Representation Learning Workshop*, 2015.

- Huang, P.-Y., Xu, H., Li, J., Baevski, A., Auli, M., Galuba, W., Metze, F., Feichtenhofer, C., et al. Masked autoencoders that listen. In *NeurIPS*, 2022a.
- Huang, Z., Jin, X., Lu, C., Hou, Q., Cheng, M.-M., Fu, D., Shen, X., and Feng, J. Contrastive masked autoencoders are stronger vision learners. *arXiv preprint arXiv:2207.13532*, 2022b.
- Jaegle, A., Gimeno, F., Brock, A., Vinyals, O., Zisserman, A., and Carreira, J. Perceiver: General perception with iterative attention. In *ICML*, 2021.
- Kazakos, E., Nagrani, A., Zisserman, A., and Damen, D. Epic-fusion: Audio-visual temporal binding for egocentric action recognition. In *ICCV*, 2019.
- Kim, Y., Lee, H., and Provost, E. M. Deep learning for robust feature generation in audiovisual emotion recognition. In *ICASSP*, 2013.
- Kong, Q., Cao, Y., Iqbal, T., Wang, Y., Wang, W., and Plumbley, M. D. PANNs: Large-scale pretrained audio neural networks for audio pattern recognition. *IEEE/ACM Transactions on Audio, Speech, and Language Processing*, 28:2880–2894, 2020.
- Korbar, B., Tran, D., and Torresani, L. Cooperative learning of audio and video models from self-supervised synchronization. *Advances in Neural Information Processing Systems*, 31, 2018.
- Koutini, K., Schlüter, J., Eghbal-zadeh, H., and Widmer, G. Efficient training of audio transformers with patchout. *arXiv preprint arXiv:2110.05069*, 2021.
- Larsson, G., Maire, M., and Shakhnarovich, G. FractalNet: Ultra-deep neural networks without residuals. In *ICLR*, 2017.
- Li, J. B., Qu, S., Huang, P., and Metze, F. AudioTagging Done Right: 2nd comparison of deep learning methods for environmental sound classification. *CoRR*, abs/2203.13448, 2022. doi: 10.48550/arXiv.2203.13448. URL <https://doi.org/10.48550/arXiv.2203.13448>.
- Li, Y., Wu, C.-Y., Fan, H., Mangalam, K., Xiong, B., Malik, J., and Feichtenhofer, C. Improved multiscale vision transformers for classification and detection. *arXiv preprint arXiv:2112.01526*, 2021.
- Liu, X., Zhou, J., Kong, T., Lin, X., and Ji, R. Exploring target representations for masked autoencoders. *arXiv preprint arXiv:2209.03917*, 2022.
- Loshchilov, I. and Hutter, F. SGDR: Stochastic gradient descent with warm restarts. In *ICLR*, 2017.
- Loshchilov, I. and Hutter, F. Decoupled weight decay regularization. In *ICLR*, 2019.
- Ma, S., Zeng, Z., McDuff, D., and Song, Y. Active contrastive learning of audio-visual video representations. In *ICLR*, 2020.
- Miech, A., Zhukov, D., Alayrac, J.-B., Tapaswi, M., Laptev, I., and Sivic, J. HowTo100M: Learning a text-video embedding by watching hundred million narrated video clips. In *ICCV*, 2019.
- Mishra, A. and Marr, D. Apprentice: Using knowledge distillation techniques to improve low-precision network accuracy. In *ICLR*, 2018.
- Mohamed, A., Lee, H.-y., Borgholt, L., Havtorn, J. D., Edin, J., Igel, C., Kirchhoff, K., Li, S.-W., Livescu, K., Maaløe, L., Sainath, T. N., and Watanabe, S. Self-supervised speech representation learning: A review. *IEEE Journal of Selected Topics in Signal Processing*, 16(6):1179–1210, 2022.
- Morgado, P., Misra, I., and Vasconcelos, N. Robust audio-visual instance discrimination. In *CVPR*, 2021a.
- Morgado, P., Vasconcelos, N., and Misra, I. Audio-visual instance discrimination with cross-modal agreement. In *CVPR*, 2021b.
- Müller, R., Kornblith, S., and Hinton, G. E. When does label smoothing help? In Wallach, H. M., Larochelle, H., Beygelzimer, A., d’Alché-Buc, F., Fox, E. B., and Garnett, R. (eds.), *Advances in Neural Information Processing Systems 32: Annual Conference on Neural Information Processing Systems 2019, NeurIPS 2019, December 8-14, 2019, Vancouver, BC, Canada*, pp. 4696–4705, 2019. URL <https://proceedings.neurips.cc/paper/2019/hash/f1748d6b0fd9d439f71450117eba2725-Abstract.html>.
- Nagrani, A., Yang, S., Arnab, A., Jansen, A., Schmid, C., and Sun, C. Attention bottlenecks for multimodal fusion. In *NeurIPS*, 2021.
- Ngiam, J., Khosla, A., Kim, M., Nam, J., Lee, H., and Ng, A. Y. Multimodal deep learning. In *ICML*, 2011.
- Owens, A. and Efros, A. A. Audio-visual scene analysis with self-supervised multisensory features. In *ECCV*, 2018.
- Park, D. S., Chan, W., Zhang, Y., Chiu, C.-C., Zoph, B., Cubuk, E. D., and Le, Q. V. SpecAugment: A simple data augmentation method for automatic speech recognition. *ArXiv*, abs/1904.08779, 2019a.
- Park, W., Kim, D., Lu, Y., and Cho, M. Relational knowledge distillation. In *CVPR*, 2019b.
- Patrick, M., Asano, Y. M., Kuznetsova, P., Fong, R., Henriques, J. F., Zweig, G., and Vedaldi, A. On compositions of transformations in contrastive self-supervised learning. In *ICCV*, 2021a.
- Patrick, M., Huang, P., Misra, I., Metze, F., Vedaldi, A., Asano, Y. M., and Henriques, J. F. Space-time crop & attend: Improving cross-modal video representation learning. In *2021 IEEE/CVF International Conference on Computer Vision, ICCV 2021, Montreal, QC, Canada, October 10-17, 2021*, pp. 10540–10552. IEEE, 2021b. doi: 10.1109/ICCV48922.2021.01039. URL <https://doi.org/10.1109/ICCV48922.2021.01039>.
- Paulus, R., Xiong, C., and Socher, R. A deep reinforced model for abstractive summarization. *arXiv*, abs/1705.04304, 2017.
- Petajan, E. D. *Automatic Lipreading to Enhance Speech Recognition (Speech Reading)*. PhD thesis, University of Illinois at Urbana-Champaign, 1984.
- Piczak, K. J. ESC: Dataset for Environmental Sound Classification. In *Proceedings of the 23rd Annual ACM Conference on Multimedia*, pp. 1015–1018. ACM Press, 2015. ISBN 978-1-4503-3459-4. doi: 10.1145/2733373.2806390. URL <http://dl.acm.org/citation.cfm?doid=2733373.2806390>.

- Potamianos, G., Neti, C., Gravier, G., Garg, A., and Senior, A. W. Recent advances in the automatic recognition of audiovisual speech. *Proceedings of the IEEE*, 91(9):1306–1326, 2003.
- Povey, D., Ghoshal, A., Boulianne, G., Burget, L., Glembek, O., Goel, N., Hannemann, M., Motlicek, P., Qian, Y., Schwarz, P., et al. The kaldi speech recognition toolkit. In *IEEE 2011 workshop on automatic speech recognition and understanding*, number CONF. IEEE Signal Processing Society, 2011.
- Radford, A., Kim, J. W., Hallacy, C., Ramesh, A., Goh, G., Agarwal, S., Sastry, G., Askell, A., Mishkin, P., Clark, J., Krueger, G., and Sutskever, I. Learning transferable visual models from natural language supervision. In *ICML*, 2021.
- Ramachandram, D. and Taylor, G. W. Deep multimodal learning: A survey on recent advances and trends. *IEEE signal processing magazine*, 34(6):96–108, 2017.
- Ramesh, A., Pavlov, M., Goh, G., Gray, S., Voss, C., Radford, A., Chen, M., and Sutskever, I. Zero-shot text-to-image generation. In Meila, M. and Zhang, T. (eds.), *Proceedings of the 38th International Conference on Machine Learning, ICML 2021, 18-24 July 2021, Virtual Event*, volume 139 of *Proceedings of Machine Learning Research*, pp. 8821–8831. PMLR, 2021. URL <http://proceedings.mlr.press/v139/ramesh21a.html>.
- Recasens, A., Luc, P., Alayrac, J.-B., Wang, L., Strub, F., Tallec, C., Malinowski, M., Pătrăucean, V., Altché, F., Valko, M., et al. Broaden your views for self-supervised video learning. In *ICCV*, 2021.
- Romero, A., Ballas, N., Kahou, S. E., Chassang, A., Gatta, C., and Bengio, Y. FitNets: Hints for thin deep nets. *ICLR*, 2015.
- Rouditchenko, A., Boggust, A., Harwath, D., Chen, B., Joshi, D., Thomas, S., Audhkhasi, K., Kuehne, H., Panda, R., Feris, R., et al. AVLnet: Learning audio-visual language representations from instructional videos. In *Interspeech*, 2021.
- Roy, D. Learning from sights and sounds: a computational model. *PhD Thesis, MIT Media Laboratory*, 1999.
- Shi, B., Hsu, W.-N., Lakhotia, K., and Mohamed, A. Learning audio-visual speech representation by masked multimodal cluster prediction. In *ICLR*, 2022.
- Tang, Z., Cho, J., Nie, Y., and Bansal, M. TVLT: Textless Vision-Language Transformer. In *NeurIPS*, 2022.
- Tian, Y., Krishnan, D., and Isola, P. Contrastive representation distillation. In *ICLR*, 2019.
- van den Oord, A., Li, Y., and Vinyals, O. Representation learning with contrastive predictive coding. *CoRR*, abs/1807.03748, 2018. URL <http://arxiv.org/abs/1807.03748>.
- Vaswani, A., Shazeer, N., Parmar, N., Uszkoreit, J., Jones, L., Gomez, A. N., Kaiser, Ł., and Polosukhin, I. Attention is all you need. *NeurIPS*, 2017.
- Wang, L., Luc, P., Recasens, A., Alayrac, J.-B., and Oord, A. v. d. Multimodal self-supervised learning of general audio representations. *arXiv preprint arXiv:2104.12807*, 2021.
- Wang, W., Tran, D., and Feiszli, M. What makes training multimodal classification networks hard? In *CVPR*, 2020.
- Warden, P. Speech Commands: A Dataset for Limited-Vocabulary Speech Recognition. *ArXiv e-prints*, April 2018. URL <https://arxiv.org/abs/1804.03209>.
- Wei, C., Fan, H., Xie, S., Wu, C.-Y., Yuille, A., and Feichtenhofer, C. Masked feature prediction for self-supervised visual pre-training. In *CVPR*, 2022a.
- Wei, L., Xie, L., Zhou, W., Li, H., and Tian, Q. MVP: Multimodality-guided visual pre-training. In *ECCV*, 2022b.
- Wei, Y., Hu, H., Xie, Z., Zhang, Z., Cao, Y., Bao, J., Chen, D., and Guo, B. Contrastive learning rivals masked image modeling in fine-tuning via feature distillation. *arXiv preprint arXiv:2205.14141*, 2022c.
- Xiao, F., Lee, Y. J., Grauman, K., Malik, J., and Feichtenhofer, C. Audiovisual slowfast networks for video recognition. *arXiv preprint arXiv:2001.08740*, 2020.
- Xu, J., Mei, T., Yao, T., and Rui, Y. MSR-VTT: A large video description dataset for bridging video and language. In *CVPR*, 2016.
- Yun, S., Han, D., Oh, S. J., Chun, S., Choe, J., and Yoo, Y. Cutmix: Regularization strategy to train strong classifiers with localizable features. In *ICCV*, 2019.
- Zeng, Z., McDuff, D., Song, Y., et al. Contrastive learning of global and local video representations. In *NeurIPS*, 2021.
- Zhang, H., Cisse, M., Dauphin, Y. N., and Lopez-Paz, D. mixup: Beyond empirical risk minimization. In *ICLR*, 2018.
- Zhou, L., Xu, C., and Corso, J. J. Towards automatic learning of procedures from web instructional videos. In *AAAI*, 2018.